สเปกโทรสโกปีการทะลุผ่านรอยต่อโลหะปรกติ-ฉนวน-ตัวนำยวดยิ่งแบบดีเวฟที่อุณหภูมิอันตะ

นายแหลมทอง ลัดดาวงศ์

TUNNELING SPECTROSCOPY OF NORMAL METAL-INSULATOR-D-WAVE SUPER-CONDUCTOR JUNCTION AT FINITE TEMPERATURES

Mr. Lemthong Lathdavong

A Thesis Submitted in Partial Fulfillment of the Requirements
for the Degree of Master of Science in Physics
Suranaree University of Technology
Academic Year 2002

TUNNELING SPECTROSCOPY OF NORMAL METAL-INSULATOR-D-WAVE SUPER-CONDUCTOR JUNCTION AT FINITE TEMPERATURES

Suranaree University of Technology has approved this thesis submitted in partial fulfillment of the requirements for a Master's Degree

Thesis Examining Committee

_____

(Dr. Worasit Uchai)
Chairman

_____

(Dr. Puangratana Pairor)
Member (Thesis Advisor)

_____

(Assoc. Prof. Dr. Samnao Phatisena)
Member

_____

(Dr. Saroj Rujirawat)
Member

_____

(Dr. Sukit Limpijumnong)
Member

_____

(Assoc. Prof. Dr. Tawit Chitsomboon)
Vice Rector for Academic Affairs

(Assoc. Prof. Dr. Prasart Suebka)
Dean of Institute of Science

แหลมทอง ลัดดาวงศ์ : สเปกโทรสโกปีการทะลุผ่านรอยต่อโลหะปรกติ-ฉนวน-ตัวนำยวดยิ่งแบบดีเวฟที่อุณหภูมิอันตะ
(TUNNELING SPECTROSCOPY OF NORMAL METAL-INSULATOR-*D*-WAVE SUPERCONDUCTOR JUNCTION AT FINITE TEMPERATURES) อ. ที่ปรึกษา: ดร. พวงรัตน์ ไพเราะ, 36 หน้า.
ISBN 974-533-195-3

วิทยานิพนธ์นี้เป็นการศึกษาเชิงทฤษฎีเกี่ยวกับสเปกตรัมความนำของการทะลุผ่านรอยต่อโลหะปรกติ-ฉนวน-ตัวนำยิ่งยวดแบบดีเวฟ ได้ศึกษาผลของการวางทิศทางระหว่างผิวและอุณหภูมิต่อสเปกตรัมความนำโดยใช้วิธีการกระเจิงที่เรียกว่ารูปนัยนิยมของ Blonder-Tinkham-Klapwidjk พบว่าการวางทิศทางในแนว (100) ให้เส้นโค้งแบบเชิงเส้นที่ความต่างศักย์ต่ำ และเพิ่มตามความต่างศักย์จนถึงค่าสูงสุดที่ช่องว่างพลังงานสูงสุด   สำหรับการวางทิศทางระหว่างผิวที่ต่างจากแนว (100) นอกจากจะปรากฏที่ช่องว่างพลังงานสูงสุดแล้ว ยังมียอดโด่งที่ความต่างศักย์เป็นศูนย์และยอดเตี้ยที่ช่องว่างพลังงานของการกระตุ้นซึ่งโมเมนตัมจะขนานกับแนวตั้งฉากระหว่างผิวส่วนที่เพิ่มเข้ามานี้ใช้ระบุกำหนดขนาดของช่องว่างพลังงานที่ตำแหน่งต่างๆ บนผิวเฟอร์มี

จะสังเกตรูปร่างของสเปกตรัมความนำได้โดยง่ายเมื่ออุณหภูมิไม่สูงนัก แต่เมื่ออุณหภูมิสูงขึ้นมากกว่าร้อยละสิบของอุณหภูมิวิกฤต รูปร่างเหล่านี้จะเลือนและยากต่อการตรวจหา อย่างไรก็ตามยอดที่ความต่างศักย์เป็นศูนย์จะยังคงสังเกตได้โดยจะกว้างออกและความสูงลดลง

สาขาวิชาฟิสิกส์ 	ลายมือชื่อนักศึกษา _____

ปีการศึกษา 2545 	ลายมือชื่ออาจารย์ที่ปรึกษา _____

The tunneling conductance spectrum of a normal metal-insulator- *d*-wave superconductor junction is studied theoretically. The effects of surface orientation and non-zero temperature on the conductance spectrum are investigated, using the scattering method, known as the Blonder-Tinkham-Klapwijk formalism. It is found that for the junction with (100) surface, the conductance curve is linear at low voltages, increases with voltages and peaks at the maximum gap. For the junction with the interface orientation away from (100) surface, in addition to the feature at the maximum gap, there is a peak at zero voltage, and a small peak at the energy gap of the excitation that has its momentum along the interface normal. The latter feature implies that the tunneling spectroscopy can be used to determine the magnitude of the energy gap at different points on the Fermi surface.

All the features of the conductance spectrum are easily observed when the temperature is not too high. When the temperature is higher than ten percent of the critical temperature, the smaller features are smeared out, thus, hard to detect. However, the zero-bias conductance peak is still observable, only that its width is broadened and its height is lowered.

School of Physics   Student _____

Academic Year 2002   Advisor _____

Acknowledgements

I would like to express my sincere gratitude to my advisor Dr. Puangratana Pairor for her guidance and support throughout the course of this study. Even though I have been working under her supervision for a short time, I have had many good experiences for which I am grateful.

I would also like to thank all the lecturers, who have taught me in all graduate courses, and Dr. Worasit Uchai, Assoc. Prof. Dr. Samnao Phatisena, Dr. Saroj Rujirawat, and Dr. Sukit Limpijumnong for being on my thesis committee.

In addition, I wish to express my special thanks to National University of Laos, Laos Government, and ADB for offering the scholarship which enable me to continue my advanced studies at Suranaree University of Technology, Thailand.

Finally, I would like to thank my wife and children for their love, support, encouragement, and patience throughout the sometimes tedious process of producing this dissertation. I cannot thank them enough.

Lemthong Lathdavong

Contents

Contents (Continued)

List of Figures

List of Figure (Continued)

Chapter I

Introduction

1.1 Motivation

During the past couple decades, high temperature superconductivity has been one of the most studied topics in the condensed matter physics community. The question of what mechanism leads to such high transition temperature (higher than 77 K) remains unsolved. Nevertheless, there are a few other questions involving the pairing symmetry that have been answered. The phase-sensitive experiments, such as tricrystal experiments, and tunneling experiments reveal that the pairing symmetry of the cooper pairs in these materials is d-wave (Wollman, D. A., et $al.$ 1993; Walker, M. B., et $al.$ 1996; Tsuei, C. C., and Kirtley, J. R. 1998; Wei, J. Y. T., et $al.$ 1998; Bang, Y., and Choi, H-Y. 2000). Their gap functions have nodes and change sign along the 45° and 135° lines in the momentum space. This property results in a linear dependence at low energies of the density of states (DOS). The linearity of the density of states at low energies leads to the power-law behaviour of many physical properties at low temperatures, such as specific heat and heat capacity (Gagnon, R. 1997; Taillefer, L., et $al.$ 1997). This behaviour is different from that of the conventional superconductors, which have low transition temperatures and isotropic energy gap. The specific heat C_V of a conventional superconductor is proportional to $e^{-(\frac{\Delta}{k_B T})}$ at low temperatures where Δ is the energy gap, k_B is the Boltzman constant, and T is the temperature. This dependence implies that there are no excitations at energies lower than Δ. Understanding the physical properties of high tem-

perature superconductors would lead to the understanding of the nature of their quasiparticle excitations. This would be a crucial step towards the understanding of the pairing mechanism.

One of the most powerful tools used to study the nature of the quasiparticle excitations of the superconductor is the tunneling spectroscopy of normal metal-insulator-superconductor (NIS) junction (Giaever, I. 1960; McMillan, W. L., and Rowell, J. M. 1969; Tanaka, Y., and Kashiwaya, S. 1995; Kashiwaya, S., *et al.* 1996; Tinkham, M. 1996; Wolf, E. L. 1986). The conductance spectrum of the junction in the low transmission limit is proportional to the local density of states of the superconductor (Tanaka, Y., *et al.* 1994; Tinkham, M. 1996; Rainer, D., *et al.* 1998). The shape of the conductance curve also depends on the symmetry of the energy gap. For the conventional isotropic s-wave superconductors, their tunneling conductance at finite temperatures is almost zero at low voltages, peaks at the gap and becomes constant at voltages larger than the gap (see Fig. 1.1).
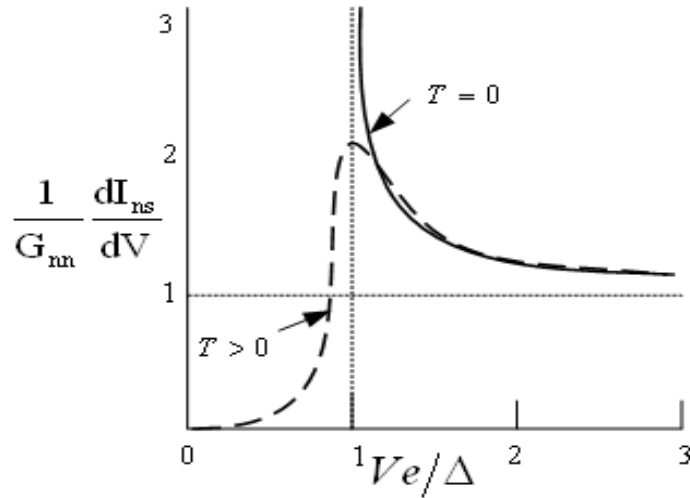
Figure 1.1: The plots of differential conductance of isotropic s-wave gap at $T = 0$ and $T > 0$. The solid curve refers to $T = 0$, and the dashed curve refers to the spectrum at finite temperatures. Note that the current at $T = 0$ is similar to the bulk DOS of superconductor. (Tinkham, M. 1996).

Because of their isotropic gap symmetry, the conductance of the isotropic s-wave superconductors does not depend on the interface orientation of the junction. However, the story is different for d-wave superconductors. Their tunneling spectroscopy depends strongly on the crystal orientation of the superconductor. As shown in Fig. 1.2, for the junction with (100) interface, the conductance as a function of applied voltage curve is linear at low voltages and peaks at the maximum of the energy gap. For the junction with (110) interface, the conductance has a peak at zero voltage but no peak at the maximum gap. The peak at zero energy for the junction with (110) interface implies the existence of a number of states at zero energy and this is a consequence of the sign change of the gap function. The zero-energy surface bound states are formed due to the change in sign of the gap function (Hu, C. R. 1994). These bound states are in fact the combination of the incoming and outgoing quasiparticle excitations, the gap functions of which have different signs. These bound states are not formed at (100) interface, because the gap functions of all incoming and outgoing excitations have the same signs.

The effect of the crystal orientation is very dramatic for d-wave superconductors. It is interesting to understand how the tunneling conductance curve would evolve with the angle between the a-axis of the crystal and the interface normal of the junction, as well as with the temperature.

1.2 Assumptions and Method

This thesis is the study of how the crystallographic orientation would affect the tunneling spectroscopy of d-wave superconductors both at zero temperature and at finite temperatures. Because all high temperature superconductors are either tetragonal, or nearly tetragonal, with the ratio of the lattice constant c to the lattice constant a bigger than 3, they will be treated as two-dimensional systems.

In the calculations throughout this thesis, the Fermi surfaces of the both
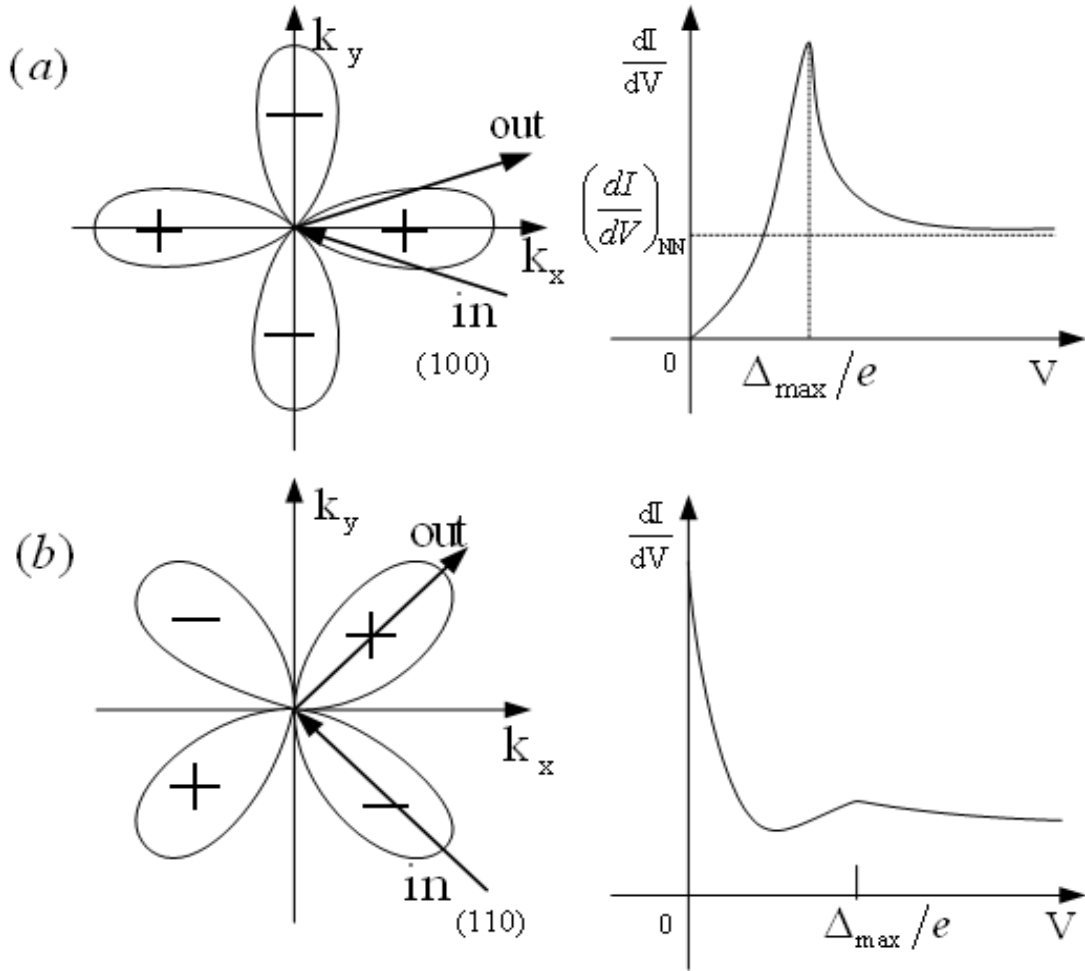
Figure 1.2: The plots of $d_{x^2-y^2}$-wave pair potential in the momentum space and the conductance spectra for 2 different crystal orientations: (a).(100) and (b).(110).

normal metal and superconductor are taken to be isotropic for simplicity. The shape of the Fermi surface should affect only the smaller features that the conductance curve may have, but not affect the main features (Pairor, P., and Walker, M. B. 2002). Also, the energy gap is taken to be zero on the normal side and finite on superconductor side and dependent only on the direction of the momentum. The proximity effect at the interface will be ignored in this thesis as well.

The method used to calculate the current across the junction in this thesis is the scattering method known as the Blonder, Thinkham and Klapwijk

(BTK) formalism (Blonder, G. E., *et al.* 1982). This method makes use of the Bogoluibov-de Gennes (BdG) equations, which are two component energy equations, and the appropriate matching conditions at the interface to obtain the reflection and transmissions coefficients, which in turn are used to calculate the current across the junction.

1.3   Outline of Thesis

This thesis consists of five chapters. In the next chapter, the current and conductance formula in the scattering method of normal metal-insulator-superconductor (NIS) junction are derived.

The conductance spectra of s-wave and d-wave superconductors at zero temperatures and at different interface orientations are then investigated in Chapter III. The evolution of the main features in the tunneling conductance spectrum of the d-wave superconductor with the orientation are examined thoroughly.

In Chapter IV, The effect of finite temperatures on the tunneling spectra will be examined and discussed. The evolution of the tunneling conductance with temperature will also be studied.

Finally, the conclusion of this work is drawn in Chapter V.

Chapter II

Current and Conductance of NIS Junction in the Isotropic Model

2.1 Introduction

The current and conductance spectra of the normal metal-insulator-superconductor (NIS) junctions in this thesis are calculated based on the assumption that the electronic structures of both superconductor and the normal metal are isotropic. Because the system of interest is either tetragonal, or nearly tetragonal, with high $\frac{c}{a}$ ratio, the Fermi surfaces for both normal metal and superconductor are taken to be cylindrical. The junction is modelled as an infinite system with the interface on the yz plane. Figure 2.1 shows the geometry of the junction. The insulator is located at the plane $x = 0$, the normal metal is on the left side ($x < 0$), and the superconductor occupies on the right side ($x > 0$). The insulating barrier is described by a delta function potential of strength H. The gap is taken to be zero in the normal side, but finite and unchanged with position in the superconductor side.
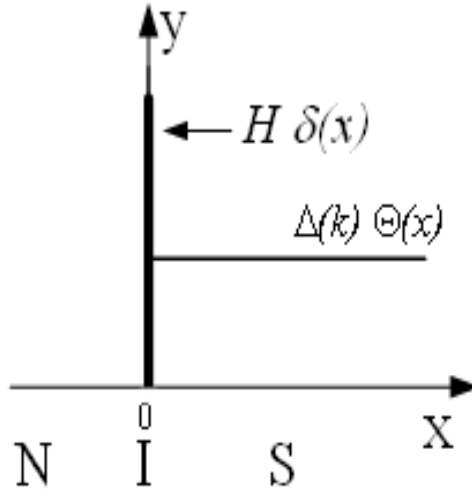
Figure 2.1: The model describes the normal metal-insulator-superconductor junction used in the thesis. The gap function is taken to be $\Delta(\vec{k})\Theta(x)$ where $\vec{k}$ is a wave vector and $\Theta(x)$ is the Heaviside step function.

2.2 The Reflection and Transmission Probabilities

The current and conductance of of the junction are calculated using the scattering method. This method starts from the Bogoluibov-de Gennes (BdG) equations and a wave function of each side (Demers, J; Griffin, A. 1971). The wave functions are later on matched at the interface with the appropriate boundary conditions to obtain the reflection and transmission probabilities.

Figure 2.2 shows the dispersion relations of the quasiparticles in a normal and superconductors. As can be seen from Fig. 2.2, for each incoming electron from normal metal side, there are two reflected excitations, which are the normal reflected and Andreev reflected (Andreev, A. F. 1964), and two transmitted excitations, which are electron-like and hole-like.
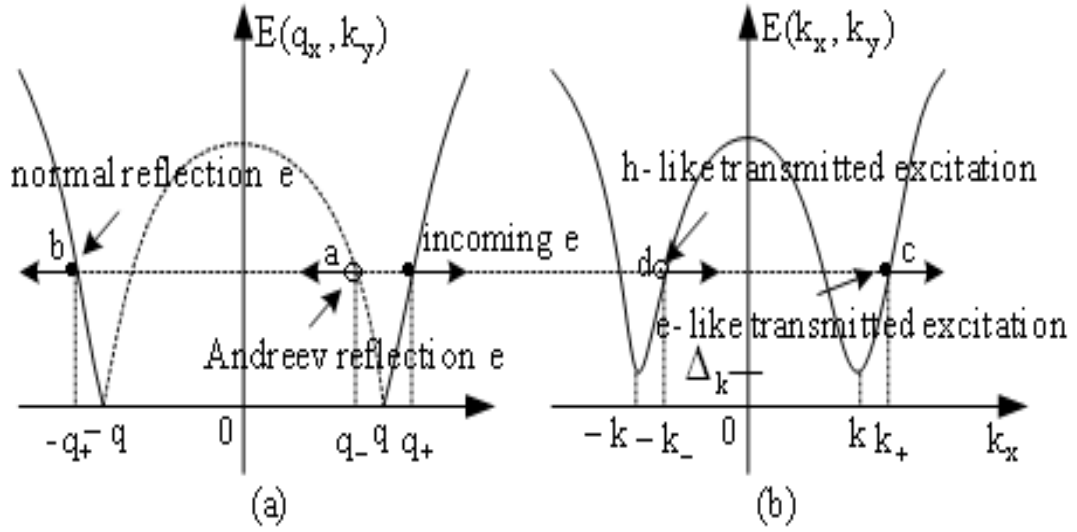
Figure 2.2: The sketches of the bulk quasi-particle energies of (a) the normal metal and (b) the superconductor.

The Bogoluibov-de Gennes (BdG) equations that described the junction are

$$[-\frac{\hbar^2}{2m}\nabla^2 - \mu]u(\vec{r}) + \Delta(\vec{r})v(\vec{r}) = Eu(\vec{r}) \ , \qquad (2.1)$$

$$\Delta^*(\vec{r})u(\vec{r}) + [\frac{\hbar^2}{2m}\nabla^2 + \mu]v(\vec{r}) = Ev(\vec{r}) \ , \qquad (2.2)$$

where $\Delta(\vec{r})$ is the pairing potential, μ is the chemical potential, m is the electron mass, and $u(\vec{r})$ and $v(\vec{r})$ denote the electron-like and hole-like components of the wave function, or

$$\psi(\vec{r}) = \left(\begin{array}{c} u(\vec{r}) \\ v(\vec{r}) \end{array} \right) . \qquad (2.3)$$

The wave function of the normal side takes the form

$$\psi_N(x < 0, y) = \psi_{inc} + \psi_{refl} \ ,$$

where

$$\psi_{inc} = \left[\begin{array}{c} 1 \\ 0 \end{array} \right] e^{i(q_+ x + k_y y)} \ ,$$

and

$$\psi_{refl} = a \begin{bmatrix} 0 \\ 1 \end{bmatrix} e^{i(q_- x + k_y y)} + b \begin{bmatrix} 1 \\ 0 \end{bmatrix} e^{-i(q_+ x - k_y y)} \ ,$$

where a, b are the amplitudes of Andreev and normal reflections, respectively. Thus

$$\psi_N(x < 0, y) = \left(\begin{bmatrix} 1 \\ 0 \end{bmatrix} e^{iq_+ x} + a \begin{bmatrix} 0 \\ 1 \end{bmatrix} e^{iq_- x} + b \begin{bmatrix} 1 \\ 0 \end{bmatrix} e^{-iq_+ x} \right) e^{ik_y y} \ . \quad (2.4)$$

The wave function of the superconductor is written as

$$\psi_S(x > 0, y) = \psi_{trans} \ ,$$

or

$$\psi_S(x > 0, y) = \left(c \begin{bmatrix} u_{k_+} \\ v_{k_+} \end{bmatrix} e^{ik_+ x} + d \begin{bmatrix} u_{-k_-} \\ v_{-k_-} \end{bmatrix} e^{-ik_- x} \right) e^{ik_y y} \ , \quad (2.5)$$

where c, d are the amplitudes of electron-like and hole-like transmitted excitations, respectively.

The bulk excitation energy of the normal metal is therefore

$$E(q_x, k_y) = \pm \left[\frac{\hbar^2}{2m}(q_x^2 + k_y^2) - \mu \right] \ , \quad (2.6)$$

and the quasiparticle energy of the superconductor in the bulk is

$$E(k_x, k_y) = \sqrt{\xi_k^2 + \triangle_k^2} \ , \quad (2.7)$$

where

$$\xi_k = [\frac{\hbar^2}{2m}(k_x^2 + k_y^2) - \mu] \ . \quad (2.8)$$

Here q_x, k_y are the x and y component of a wave vector.

The u_k, v_k in the Eq. (2.5) are

$$u_k = \frac{E + \xi_k}{\sqrt{|E + \xi_k|^2 + |\triangle_k|^2}} \ ,$$

$$v_k = \frac{\triangle_k}{\sqrt{|E + \xi_k|^2 + |\triangle_k|^2}} \ .$$

Note that $|u_k|^2 + |v_k|^2 = 1$.

The amplitudes of the a, b, c, d can be found by the matching conditions at the interface. The appropriate conditions for the two wave functions are the continuity of the two wave functions at $x = 0$:

$$\psi_S \Big|_{x=0^+} = \psi_N \Big|_{x=0^-} , \tag{2.9}$$

and the discontinuity of their derivatives at boundary, that is

$$\frac{\partial \psi_S}{\partial x} \Big|_{x=0^+} - \frac{\partial \psi_N}{\partial x} \Big|_{x=0^-} = \frac{2mH}{\hbar^2} \psi_S \Big|_{x=0^+} . \tag{2.10}$$

With these two boundary conditions, the amplitudes of reflections and transmissions can be found from the equation:

$$\begin{bmatrix} -1 & 0 & v_{k_+} & v_{-k_-} \\ 0 & -1 & u_{k_+} & u_{-k_-} \\ 0 & 0 & u_{k_+}(ik_+ + iq_+ - 2Zk_F) & u_{-k_-}(iq_+ - ik_- - 2Zk_F) \\ 0 & 0 & v_{k_+}(ik_+ - iq_- - 2Zk_F) & -v_{-k_-}(iq_- + ik_- + 2Zk_F) \end{bmatrix} \begin{bmatrix} a \\ b \\ c \\ d \end{bmatrix} = \begin{bmatrix} 0 \\ 1 \\ 2iq_+ \\ 0 \end{bmatrix} . \tag{2.11}$$

The dimensionless parameter $Z \equiv \frac{mH}{\hbar^2 k_F}$ represents the strength of the barrier in this equation.

For $\Delta \ll E_F$, the following approximation can be made: $q_- \approx q_+ \approx q_x$, where $q_x = \sqrt{q_F^2 - k_y^2}$, and $k_- \approx k_+ \approx k_x$, where $k_x = \sqrt{k_F^2 - k_y^2}$.

Therefore, the reflection and transmission amplitudes can be found as

$$a = \frac{4 v_{k_+} v_{-k_-} q_x k_x}{(u_{k_+} v_{-k_-})[(k_x + q_x)^2 + 4Z^2 k_F^2] - (u_{-k_-} v_{k_+})[(q_x - k_x)^2 + 4Z^2 k_F^2]} ,$$

$$b = \frac{(v_{k_+} u_{-k_-} - v_{-k_-} u_{k_+})[(q_x^2 - k_x^2) - 4izq_x - 4Z^2 k_F^2]}{(u_{k_+} v_{-k_-})[(k_x + q_x)^2 + 4Z^2 k_F^2] - (u_{-k_-} v_{k_+})[(q_x - k_x)^2 + 4Z^2 k_F^2]} ,$$

$$\qquad\qquad\qquad\qquad\qquad\qquad\qquad\qquad\qquad\qquad\qquad\qquad\qquad\qquad\qquad\qquad\qquad \tag{2.12}$$

$$c = \frac{2 q_x v_{-k_-}[(k_x + q_x) - 2iZk_F]}{(u_{k_+} v_{-k_-})[(k_x + q_x)^2 + 4Z^2 k_F^2] - (u_{-k_-} v_{k_+})[(q_x - k_x)^2 + 4Z^2 k_F^2]} ,$$

$$d = \frac{2 q_x v_{k_+}[(k_x - q_x) - 2iZk_F]}{(u_{k_+} v_{-k_-})[(k_x + q_x)^2 + 4Z^2 k_F^2] - (u_{-k_-} v_{k_+})[(q_x - k_x)^2 + 4Z^2 k_F^2]} .$$

If θ is the angle between the Fermi wave vector and the x-axis, the wave

vector $k_x = k_F \cos\theta$, and the reflection and transmission amplitudes become

$$a = \frac{4\lambda v_{k_+} v_{-k_-} \cos^2\theta}{(u_{k_+} v_{-k_-})[(1+\lambda)^2 \cos^2\theta + 4Z^2] - (u_{-k_-} v_{k_+})[(\lambda-1)^2 \cos^2\theta + 4Z^2 k_F^2]} \ ,$$

$$b = \frac{(v_{k_+} u_{-k_-} - v_{-k_-} u_{k_+})[(\lambda^2-1)\cos^2\theta - 4i\lambda Z \cos\theta - 4z^2]}{(u_{k_+} v_{-k_-})[(1+\lambda)^2 \cos^2\theta + 4Z^2] - (u_{-k_-} v_{k_+})[(\lambda-1)^2 \cos^2\theta + 4Z^2 k_F^2]} \ ,$$

$$c = \frac{2\lambda v_{-k_-} \cos\theta[(1+\lambda)\cos\theta - 2iZ]}{(u_{k_+} v_{-k_-})[(1+\lambda)^2 \cos^2\theta + 4Z^2] - (u_{-k_-} v_{k_+})[(\lambda-1)^2 \cos^2\theta + 4Z^2 k_F^2]} \ ,$$

$$d = \frac{2\lambda v_{k_+} \cos\theta[(\lambda-1)\cos\theta - 2iZ]}{(u_{k_+} v_{-k_-})[(1+\lambda)^2 \cos^2\theta + 4Z^2] - (u_{-k_-} v_{k_+})[(\lambda-1)^2 \cos^2\theta + 4Z^2 k_F^2]} \ ,$$

$$(2.13)$$

where $\lambda = \frac{q_F}{k_F}$.

The reflection probability is equal to the magnitude of the ratio between the current density of the reflected excitation and that of the incident excitation.

$$\left| \frac{J_{refl}}{J_{inc}} \right| = \left| \frac{\psi_R^\dagger \psi_R v_g^{refl}}{\psi_I^\dagger \psi_I v_g^{inc}} \right| \ , \tag{2.14}$$

where $\psi^\dagger$ is the adjoint of the wave function ψ, v_g^{refl} and v_g^{inc} are the group velocities of the reflected and incident excitation, respectively. Therefore, the Andreev reflection probability $A(E,\theta)$ is equal to

$$A(E,\theta) = |a(E,\theta)|^2 \left| \frac{q_x^+}{q_x^-} \right| \approx |a(E,\theta)|^2 \ , \tag{2.15}$$

and by the same token the normal reflection probability $B(E,\theta)$ is

$$B(E,\theta) \approx |b(E,\theta)|^2. \tag{2.16}$$

The transmission probability is defined as

$$\left| \frac{J_{Tran}}{J_{inc}} \right| = \left| \frac{\psi_{Tr}^\dagger \psi_{Tr} v_g^{Tr}}{\psi_I^\dagger \psi_I v_g^{inc}} \right| \ , \tag{2.17}$$

where v_g^{Tr} is the group velocity of either transmitted electron-like or hole-like quasiparticle. Thus, the transmission probability of the electron-like quasiparticle $C(E,\theta)$ is equal to

$$C(E,\theta) = |c(E,\theta)|^2 \left(|u_{k^+}|^2 - |v_{k^+}|^2 \right) \left| \frac{k_x^+}{q_x^-} \right|$$

$$\Rightarrow C(E,\theta) \approx |c(E,\theta)|^2 \left(|u_{k^+}|^2 - |v_{k^+}|^2 \right) \frac{1}{\lambda} \ , \tag{2.18}$$

and similarly the transmission probability of the hole-like quasiparticle $D(E, \theta)$ is

$$D(E, \theta) \approx |d(E, \theta)|^2 \left(|u_{k^+}|^2 - |v_{k^+}|^2 \right) \frac{1}{\lambda} \ . \tag{2.19}$$

Note that, the conservation of the coefficient probability required that

$$A(E) + B(E) + C(E) + D(E) = 1 \ .$$

In the case of the superconductor become normal metal i.e, $T > T_c$, the Andreev reflection $A(E, \theta) = 0$, and the amplitude of reflection and transmission $b(\theta)$ and $c(\theta)$ for the system would be

$$b(\theta) = \frac{i(\lambda - 1) \cos \theta + 2Z}{i(\lambda + 1) \cos \theta - 2Z} \ ,$$
$$c(\theta) = \frac{2i\lambda \cos \theta}{i(1 + \lambda) \cos \theta - 2Z} \ . \tag{2.20}$$

Thus, in the case of normal metal-insulator-normal metal junction, the probabilities of reflection and transmission are

$$B(\theta) = \frac{(\lambda - 1)^2 \cos^2 \theta + 4Z^2}{(1 + \lambda)^2 \cos^2 \theta + 4Z^2} \ ,$$
$$C(\theta) = \frac{4\lambda^2 \cos^2 \theta}{(1 + \lambda)^2 + 4Z^2 \sec^2 \theta} \ . \tag{2.21}$$

Notice that both probabilities do not depend on E.

2.3 The Current and Conductance Formula

2.3.1 The Current

The current across the junction can be calculated from the reflection and transmission coefficients. In a two dimensional system, the tunneling current is a sum of charge and group velocity products of all states $\vec{k} \simeq (k_x, k_y)$ of energy E_k that have positive group velocities v_k, therefore the current can be written as

$$I = \sum_{k_x, k_y} n_k e v_k \ , \tag{2.22}$$

where $n_k = [1 + A(E) - B(E)]f(E)$ is the number of electrons moving across the junction($f(E)$ is the Fermi-Dirac distribution function) and $v_{k_x} = \frac{1}{\hbar}\frac{dE}{dk_x}$ is the group velocity in the $+x$ direction.

When there is no applied voltage across the junction, the current to the right is equal to the current to the left, so that there is no net current across a junction. The magnitude of the current to the left and to the right is

$$I^{\rightarrow} = I^{\leftarrow} = \frac{L^2 e}{4\pi^2\hbar^2} \int_{-\infty}^{+\infty} dk_y \int_{-\infty}^{+\infty} dE(1 + A(E) - B(E))f(E) \ . \qquad (2.23)$$

However, when the voltage across V becomes non-zero, the current to the right becomes

$$I^{\rightarrow} = \frac{L^2 e}{4\pi^2\hbar^2} \int_{-\infty}^{+\infty} dk_y \int_{-\infty}^{+\infty} dE(1 + A(E) - B(E))f(E - eV) \ . \qquad (2.24)$$

Therefore, the net current at this voltage is

$$\begin{aligned}
I_{net} = I_{NIS} &= I^{\rightarrow} - I^{\leftarrow} \\
&= \frac{L^2 e}{4\pi^2\hbar^2} \int_{-\infty}^{+\infty} dk_y \int_{-\infty}^{+\infty} dE(1 + A(E) - B(E))(f(E - eV) - f(E)) \ ,
\end{aligned} \qquad (2.25)$$

or,

$$I_{NIS}(eV, T = 0) = \frac{L^2 e}{4\pi^2\hbar^2} \int dE \int dk_y(1 + A(k_y, eV) - B(k_y, eV)) \ . \qquad (2.26)$$

Define the normalized current I as the ratio of the current across NIS junction to that across NIN junction

$$I = \frac{\int_{-\infty}^{+\infty} dk_y \int \sigma_S \ dE}{\int_{-\infty}^{+\infty} dk_y \int \sigma_N \ dE} \ . \qquad (2.27)$$

where $\sigma_S = 1 + A(k_y, eV) - B(k_y, eV)$ and $\sigma_N = 1 - B(k_y)$. Write $k_y = k_F \sin\theta$, where $-\pi/2 < \theta < \pi/2$ is the angle between the x-axis and the wave vector $\vec{k}$. Therefore, the Eq. (2.27) becomes

$$I = \frac{\int dE \int_{-\pi/2}^{+\pi/2} d\theta \ \sigma_S \cos\theta}{\int dE \int_{-\pi/2}^{+\pi/2} d\theta \ \sigma_N \cos\theta} \ . \qquad (2.28)$$

2.3.2 The Conductance Spectra

The normalized conductance is defined as the ratio of the conductance of the NIS junction to the conductance of the NIN junction:

$$G = \frac{G^{NIS}}{G^{NIN}} \ , \qquad (2.29)$$

where $G^{NIS} = \frac{dI_{NIS}}{dV}$ and $G^{NIN} = \frac{dI_{NIN}}{dV}$.

Thus, the normalized conductance is

$$G(eV) = \frac{\int dE \int_{-\pi/2}^{+\pi/2} d\theta [1 + A(\theta, E) - B(\theta, E)] \ \cos\theta \ \frac{\partial f}{\partial V}(E - eV)}{\int dE \int_{-\pi/2}^{+\pi/2} d\theta \ \sigma_N \ \cos\theta \ \frac{\partial f}{\partial V}(E - eV)} \ . \qquad (2.30)$$

The expressions in Eq. (2.28) and (2.30) for both normalized current and conductance are used throughout this thesis.

In the next two chapters, the results of the calculated normalized conductances of s-wave and d-wave superconductors at zero and finite temperatures will be presented. All the plots of the normalized current and conductance as a function of applied voltage are done using Eq. (2.28) and (2.30)

Chapter III

Tunneling Spectroscopy at Zero Temperature

3.1 Introduction

Before discussing about finite temperature tunneling spectroscopy, it is always useful to examine the tunneling spectroscopy at zero temperature. In the next section, the tunneling spectroscopy of isotropic s-wave superconductors is reviewed. After that the tunneling spectroscopy of d-wave superconductors is thoroughly examined in Section 3.3. Its dependence on the interface orientation is the main focus in this Section.

In the calculation of the tunneling current and conductance spectra throughout this chapter, the Fermi wave vectors of both normal and superconductor are taken to have the same magnitude, or $\lambda = 1$ for simplicity. The different magnitudes between the Fermi wave vectors from both sides has the same effect as increasing the strength of the insulating barrier.

3.2 Isotropic s-wave Superconductor

Isotropic s-wave superconductors have isotropic energy gaps, as shown in Fig. 3.1. This means the gaps of both transmitted excitations have the same value, i.e., $\Delta_{\pm k} = \Delta_0$.
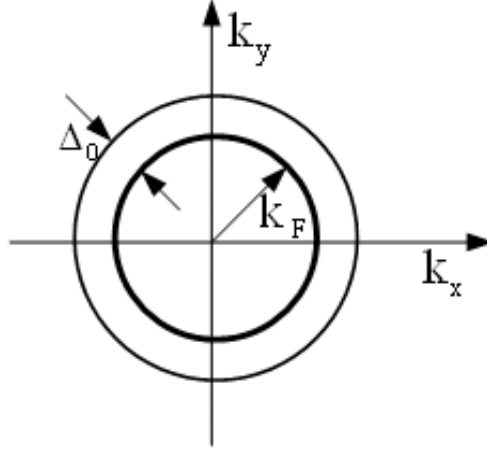
Figure 3.1: The sketch of an isotropic Fermi surface (thick circle) of the system with an isotropic s-wave gap Δ_0.

The plot of all transmission and reflection probabilities $A(E), B(E), C(E)$ and $D(E)$ in this case are illustrated in Fig. 3.2. The parameter Z represents the barrier strength at the interface.

When the barrier is weak (small Z), the normal reflection and both transmission probabilities are small for $E < \Delta_0$. The most probable process causing the current across the junction is the Andreev reflection. This process would result in two electrons tunneling across the interface (Andreev, A. F. 1964). Andreev reflection probability is high in the high transmission limit. For $E > \Delta_0$, the probability of transmission without branch crossing is dominated. Electrons tend to tunnel to the electron-like excitation states, when the barrier is weak.

When the barrier is strong (large Z), the normal reflection dominates for all energy ranges. However, it should be noted that at $E = \Delta_0$, only Andreev reflection is allowed. $A(E = \Delta_0)$ equals to 1 for all Z. Note that $A(E) + B(E) + C(E) + D(E)$ equals to 1.
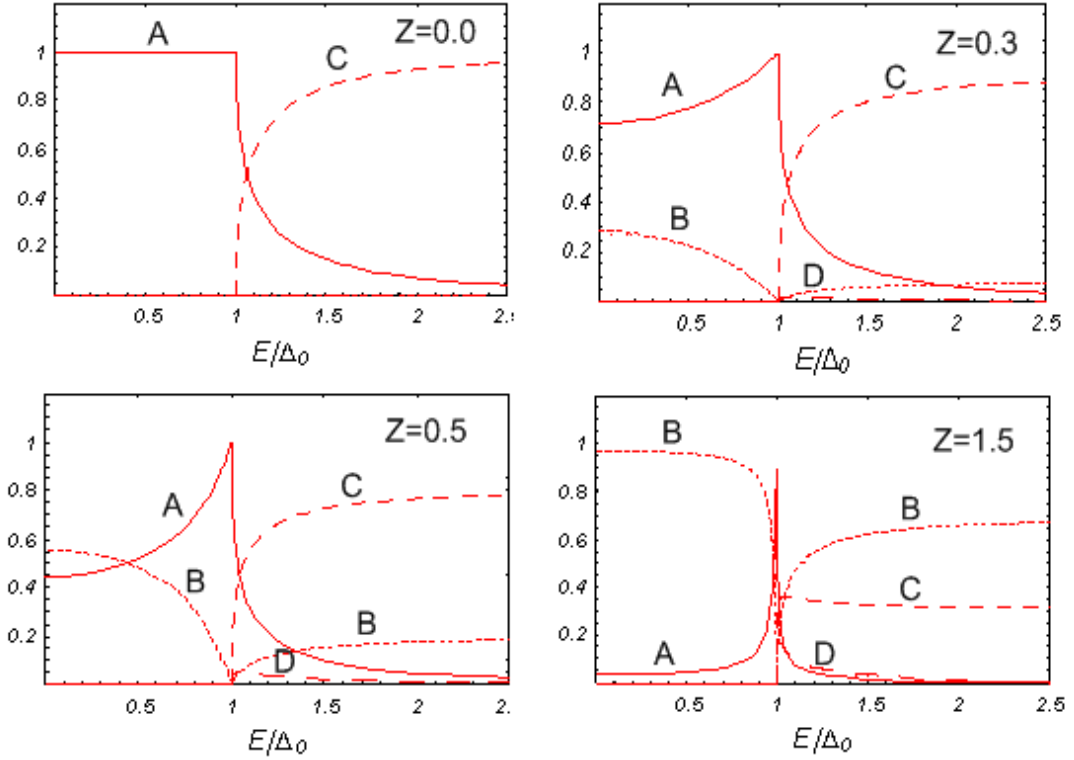
Figure 3.2: Plot of the reflection and transmission coefficients A, B, C and D at different barrier strengths (Z= 0.0, 0.3, 0.5, and 1.5).

At zero temperature the normalized current is

$$I(eV) = \frac{\int_0^{eV} dE \int dk_y [1 + A(E) - B(E)]}{eV \int dk_y (1 - B)}. \tag{3.1}$$

The $I - V$ curves for various barrier strengh Z are depicted in Fig. 3.3. For the junctions with Z=0.0, the slope of the current when $Ve < \Delta_0$ is twice the slope of the current when $Ve > \Delta_0$.

In the case of larger Z, there is almost no current when $Ve < \Delta_0$. When $Ve > \Delta_0$, the current starts to flow and reach the Ohm's law limit when the applied voltage is high.
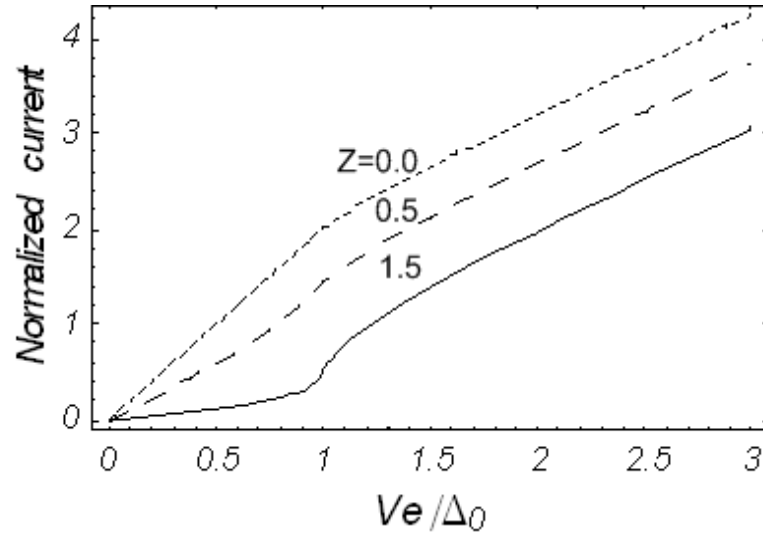
Figure 3.3: Plots of the normalized current at diferent barrier strengths.

The corresponding normalized conductance curves are shown in Fig. 3.4. In the tunneling limit, or the case of large Z, the conductance curves have the same shape on the bulk DOS of the superconductor. In the high transmission limit, or small Z, because the Andreev reflection dominates when $E < \Delta_0$, the normalized conductance can be larger than one. This reflects the fact that there can be two electrons transmitted across the junction per one incident electron, *via* the Andreev reflection process.
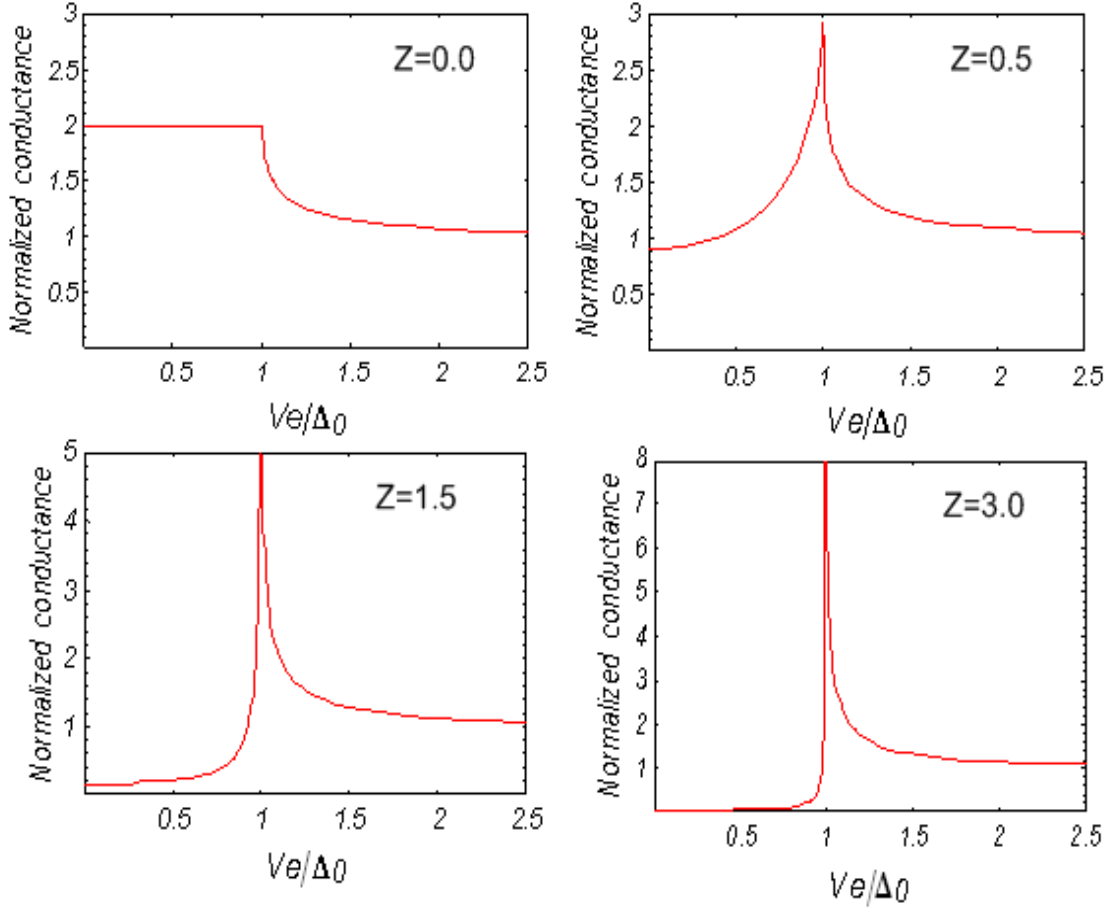
Figure 3.4: The plots of the normalized conductance vs applied voltage at different barrier strengths (Z= 0.0, 0.5, 1.5, and 3.0).

3.3 d-wave Superconductor

The gap function of the d-wave superconductor has the form

$$\Delta(k) = \Delta_0(\cos k_x - \cos k_y). \tag{3.2}$$

It can be positive or negative number and has four-node shape in k space. Let θ be the angle between the wave vector on the Fermi surface and the x-axis, and α be the angle between the a-axis of the superconductor and the x-axis, the gap function in Eq. (3.2) can be written in the following form

$$\Delta(\theta) = \Delta_{max} \cos[2(\theta - \alpha)]. \tag{3.3}$$

where $\Delta_{max} = \frac{\Delta_0 k_F^2}{2}$. Figure 3.5.(a) shows all the reflection and transmission processes occurring at the normal metal-insulator-superconductor interface. In this picture, the vertical line along the y-axis represents the insulator, and the arrows illustrate the processes. Figure 3.5.(b) show the Fermi wave surface and the gaps in two cases. The dashed curves represents the gap in the case where the a-axis is along the x-axis and the thick solid curve represents the gap in the case when the a-axis makes an angle α with the x-axis.
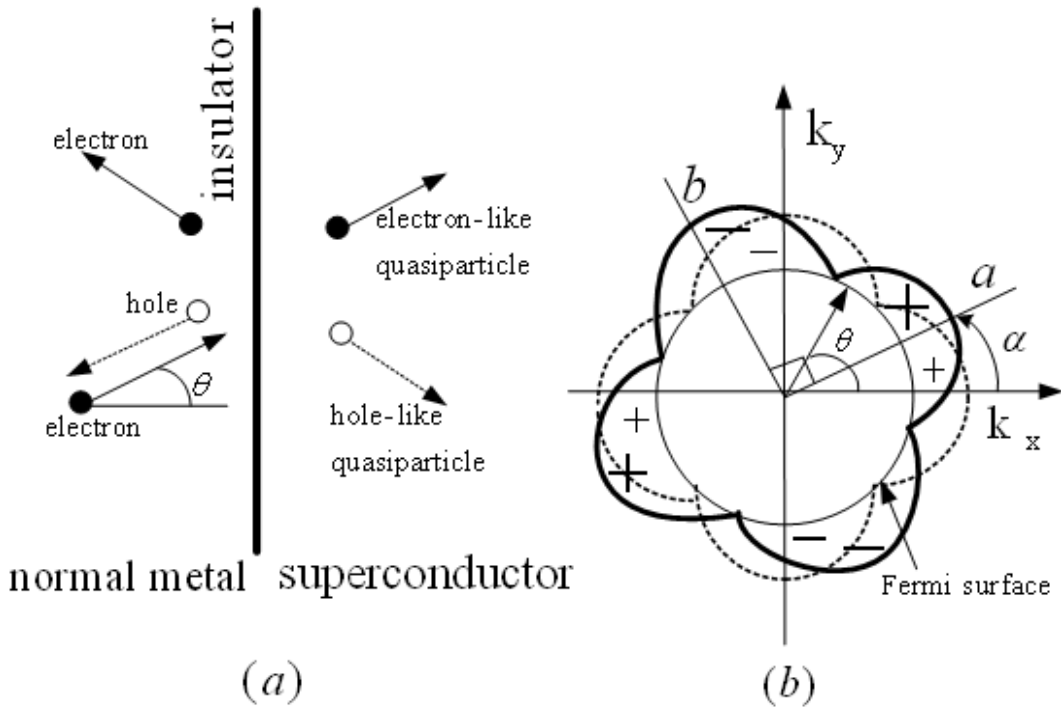
Figure 3.5: (a) The transmission and reflection processes at the junction. (b) the Fermi surface and the energy gaps in two cases.

The plots of the energy gaps of the two transmitted excitation $(k^+, -k^-)$ for different surface orientations are shown in Fig. 3.6. For $\alpha = 0$, $\Delta_{k^+} = \Delta_{-k^-}$. For $\alpha \neq 0$, Δ_{+k} is different from Δ_{-k^-}. They both sometimes have the same signs but sometime do not. For $\alpha = \frac{\pi}{4}$, they both have different signs for all values of θ.

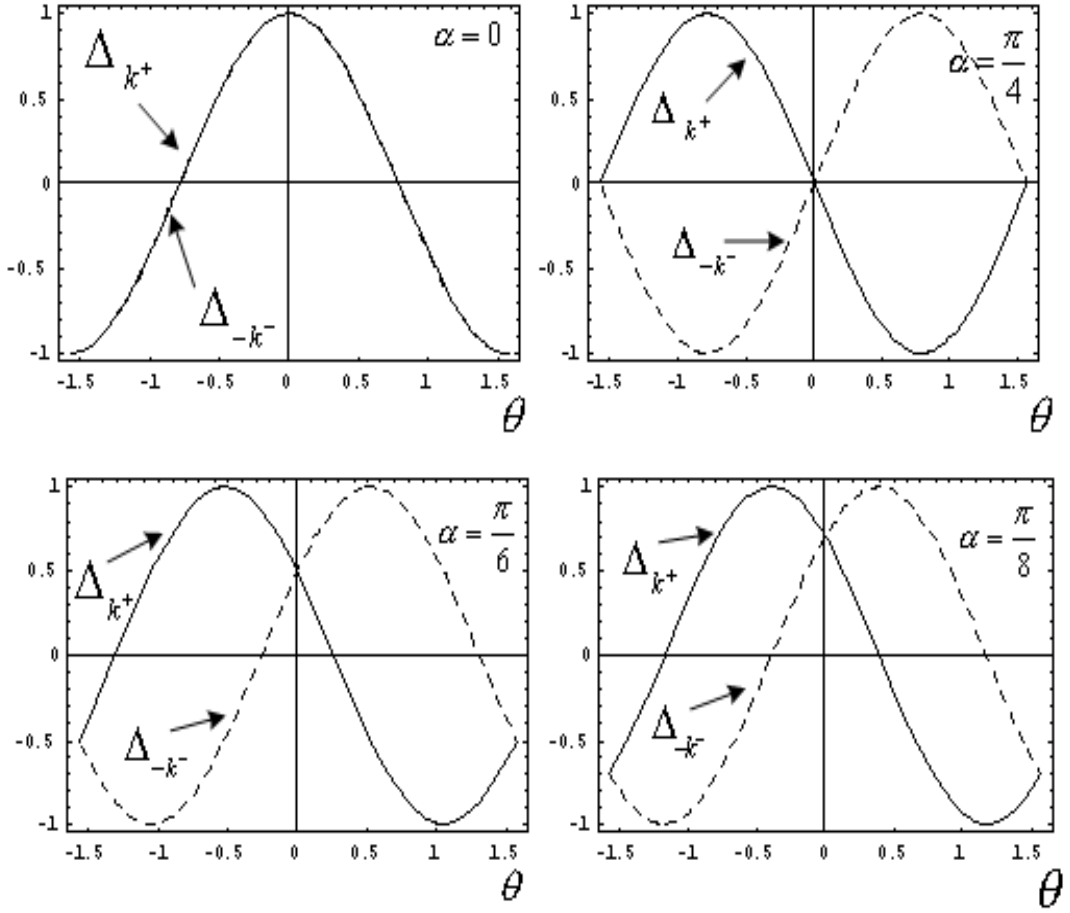Figure 3.6: The energy gaps of both transmitted excitation for different angles α. The solid lines represent Δ_{-k} and the dash line represents Δ_{+k}.

The plots of the reflection and transmission probabilities are illustrated in Fig. 3.7 and 3.8 with parameter Z=1.5. When $\alpha = 0$ (Fig. 3.7(a)), the features of each probability are similar to those in the isotropic s-wave superconductor case, only that the main feature like the peak in $A(E)$ now occurs at the energy gap of the excitations with the momentum that makes an angle θ with the a-axis. When $\alpha = \pi/4$, as shown Fig. 3.7(b), the peak of Andreev reflection appears at zero energy. This peak is the signature of the formation of zero-energy surface bound state. Both transmission probabilities start to be non-zero at the energy gap of the excitations with the momentum that makes an angle θ with the x-axis as well.

The plot of each probability in the case of different angles θ, and the angle $\alpha \neq 0$ is shown in Fig. 3.8. When θ is in the region where the two gaps (Δ_{-k-} and Δ_{k+}) have the same sign, there is no sharp peak in $A(E)$ any more. There is a broader feature which starts at $\Delta_{k+}(\theta)$ and ends at $\Delta_{-k-}(\theta)$. When θ is in the range where the two gaps have different sign, there is a peak at zero energy in $A(E)$ as well as two features occurring at $\Delta_{k+}(\theta)$ and $\Delta_{-k-}(\theta)$.
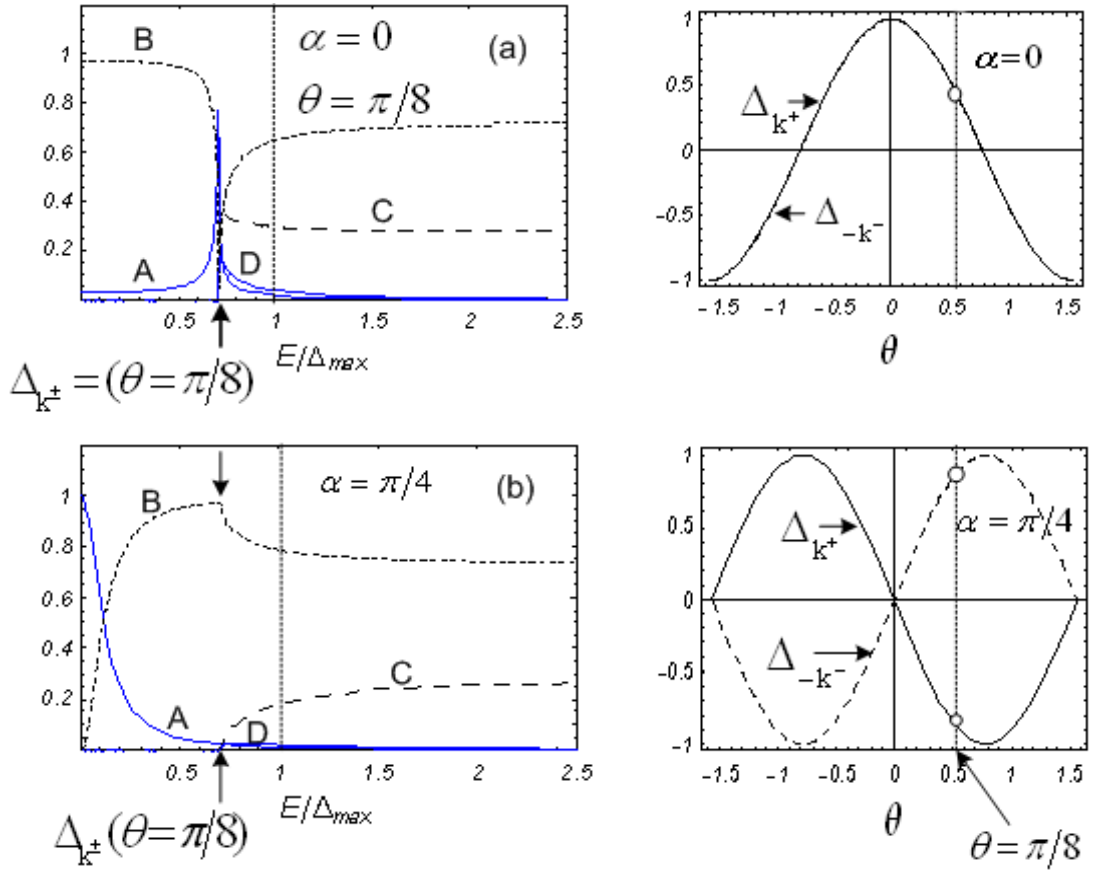

Figure 3.7: Plots of the reflection and transmission coefficients A, B, C and D for (a) $\alpha = 0$ and (b) $\alpha = \pi/4$ with $\theta = \pi/8$ and the strength of barrier Z=1.5.
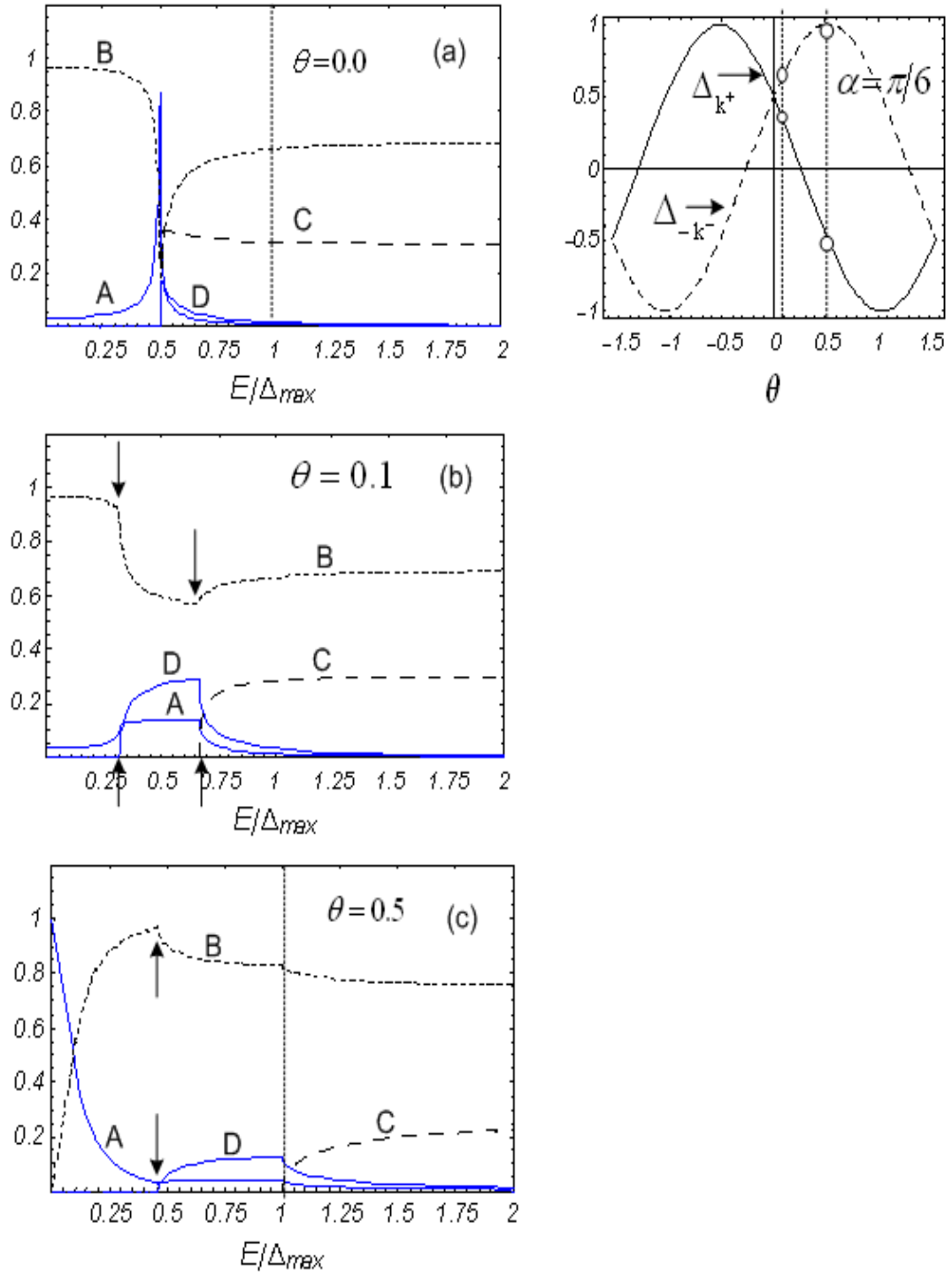
Figure 3.8: The plots of reflection and transmission coefficient A, B, C and D for (a) $\theta = 0.0$, (b) $\theta = 0.1$ and (c) $\theta = 0.5$ with $\alpha = \pi/6$ and the strength of barrier Z=1.5.
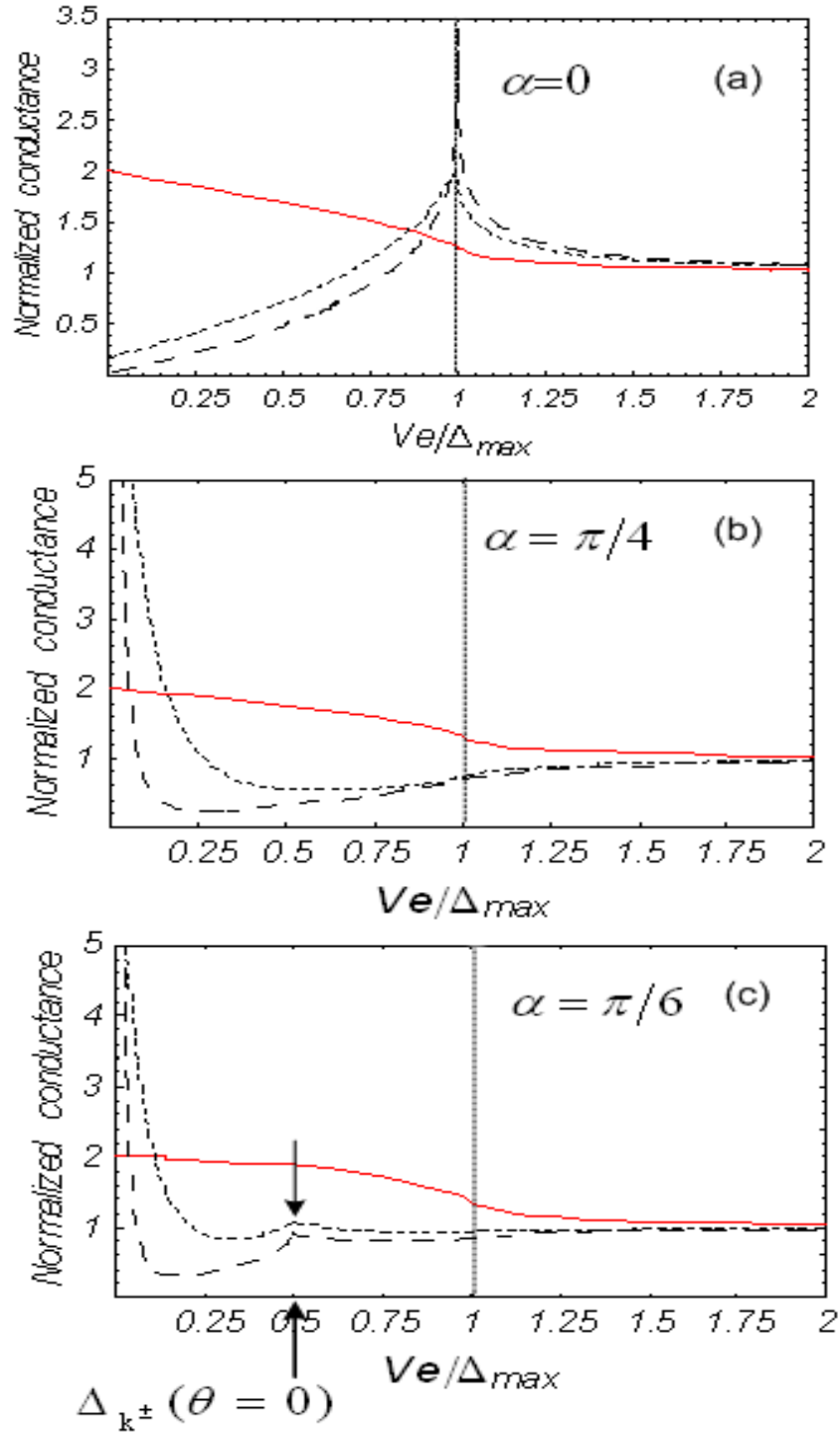
Figure 3.9: The plots of normalized conductance with different angle $\alpha = 0, \pi/4$, $\pi/6$ for: Z=0.0 (solid line), Z=1.5 (dotted line) and Z=5.0 (dashed line).
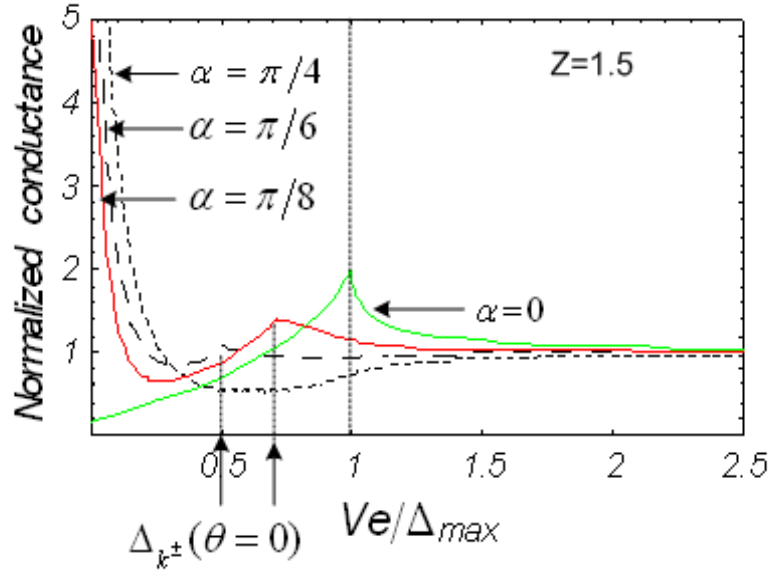
Figure 3.10: The plots of normalized conductance with different angle $\alpha = 0$, $\pi/4$, $\pi/6$, $\pi/8$ for Z=1.5.

The calculation of the tunneling conductance for $d_{x^2-y^2}$-wave superconductor junction is done using the Eq. (2.30), which is

$$G(eV) = \frac{\int dE \int_{-\pi/2}^{+\pi/2} d\theta [1 + A(\theta, E) - B(\theta, E)] \, \cos\theta \, \frac{\partial f}{\partial V}(E - eV)}{\int dE \int_{-\pi/2}^{+\pi/2} d\theta \, \sigma_N \, \cos\theta \, \frac{\partial f}{\partial V}(E - eV)}. \quad (3.4)$$

The plots of the normalized conductance as a function of energy at zero temperature and at different angle α are show in Fig. 3.9. When $\alpha = 0$, there is a main feature at $Ve = \Delta_{max}$. For Z= 0.0, the conductance has an inverted gap structure. For large Z, there is a peak at Δ_{max}. When $\alpha = \pi/4$, there is a zero-bias conductance peak. When $\alpha \neq 0$, there are two features at $Ve = \Delta_{k^\pm}(\theta = 0)$.

Figure 3.10, shows the plots of normalized conductance spectra with the strength of barrier Z= 1.5, and different angles α. It can be seen that the smaller peak (indicated by the arrows in the picture) moves when α is changed. This peak occurs at the energy gap of the excitation that has its momentum parallel to the x-axis. This implies that the NIS tunneling spectroscopy can be used to determined the magnitude of the energy gap topology on the Fermi surface.

Chapter IV

Tunneling Spectroscopy at Finite Temperatures

4.1 Introduction

The magnitude of the energy gap depends on the temperature. At zero temperature, it is maximum. As the temperature rises, magnitude gets smaller and goes to zero at T_c. From the BCS theory (Bardeen., *et al.* 1957; Parks, R. D. 1969; Thinkham, M. 1996)

$$|\Delta(T)| = |\Delta(0)| \left(1 - \sqrt{\frac{2\pi k_B T}{|\Delta(0)|}} \; exp[\frac{-|\Delta(0)|}{k_B T}]\right) \quad , \quad (T \gtrsim 0) , \qquad (4.1)$$

and

$$\frac{\Delta(T)}{\Delta(0)} \approx 1.74 \left(1 - \frac{T}{T_c}\right)^{1/2} \quad , \quad T \approx T_c , \qquad (4.2)$$

where $\Delta(0)$ is the gap at zero temperature which is equal to $1.764 k_B T_c$, and $k_B = 1.380662 \times 10^{-23} JK^{-1}$ is Boltzmann's constant. The plot of $\Delta(T)$ in BCS theory is shown in Fig. 4.1 .

In the case of anisotropic $d_{x^2-y^2}$-wave superconductor the gap function at finite temperatures takes the form

$$\Delta(T, \theta) = \Delta(T) \cos[2(\theta - \alpha)], \qquad (4.3)$$

where $\Delta(T)$ is taken from the BCS theory, α is an angle orientation between a-axis and x-axis, and θ is the angle between the incident electron direction and the

x-axis as defined previously. Note that only the magnitude of the maximum gap depends on temperature. Therefore, all the calculations done at finite temperatures are the same as all those done at zero temperature, expect the magnitude of the maximum gap is varied.

The normalized conductance formula at finite temperature is

$$G(eV) = \frac{\int dE \int_{-\pi/2}^{+\pi/2} d\theta [1 + A(\theta, E) - B(\theta, E)] \, \cos\theta \, \frac{\partial f}{\partial V}(E - eV)}{\int dE \int_{-\pi/2}^{+\pi/2} d\theta \, \sigma_N \, \cos\theta \, \frac{\partial f}{\partial V}(E - eV)} \, , \qquad (4.4)$$

where σ_N is the conductance of normal metal-insulator-normal metal.
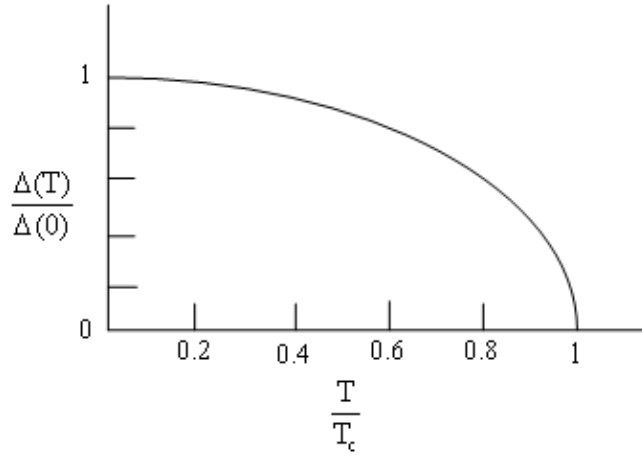

Figure 4.1: The plots of the temperature dependence of the energy gap in the BCS theory (Tinkham, M. 1996).

4.2 Isotropic s-wave Superconductor

The conductance spectra of isotropic s-wave superconductors are calculated from Eq. (4.4), the results are shown in Fig. 4.2. The features seen at zero temperature are also observed at $T \neq 0$, but they are broadened and smeared out.
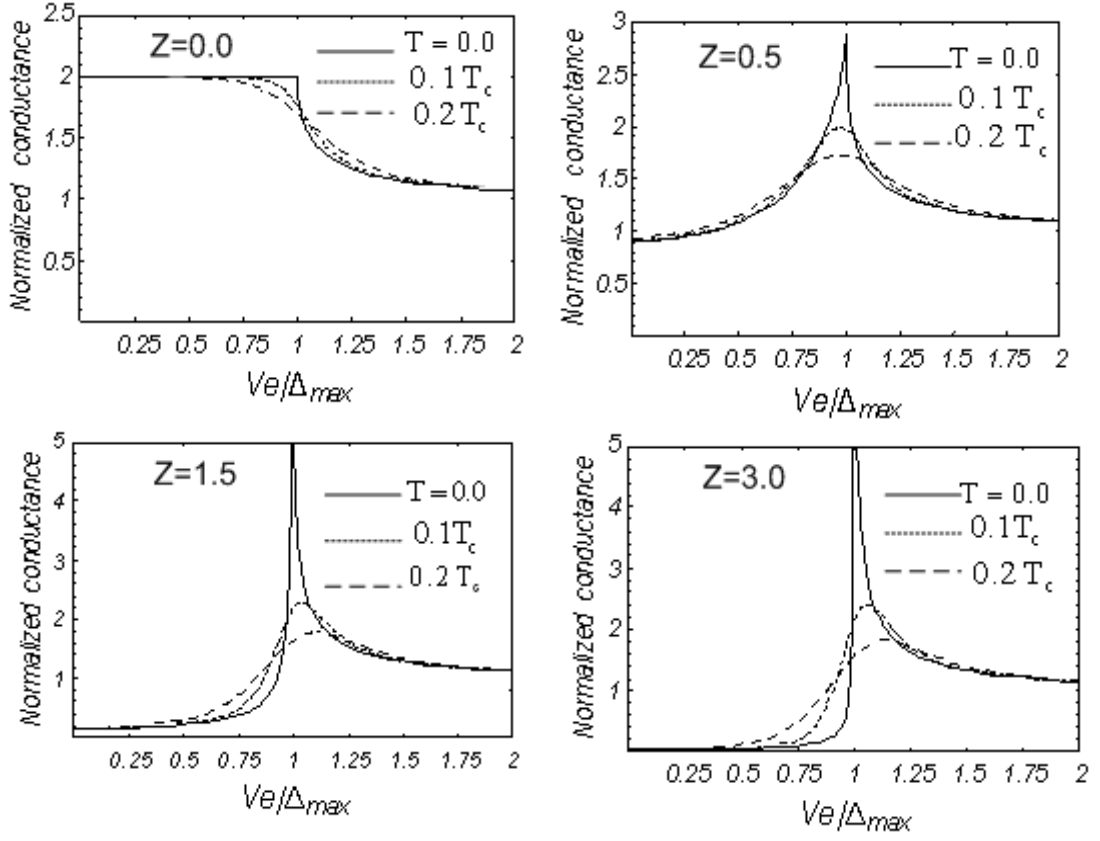
Figure 4.2: The plots of the normalized conductance at different temperature $T = 0.0$, $0.1T_c$, $0.2T_c$ and with different strength barrier Z=0.0, 0.5, 1.5, 3.0.

4.3 d-wave Superconductor

The conductance spectra in this case are calculated in the same way as in the previous section. Figure 4.3 shows the plots of normalized conductance at different temperatures and the angle α when the strength barrier is high. All the features in the conductance spectrum become broadened at high temperatures and the smaller features are smeared out. The width of the zero-bias conductance peak is broadened when the temperature is increased and the height of the peak is also decreased. The smearing behavior at finite temperatures suggests that if one wants to use the tunneling spectroscopy to measure the magnitude of the gap on the Fermi surface, one needs to do the experiment at $T < 0.1T_c$.
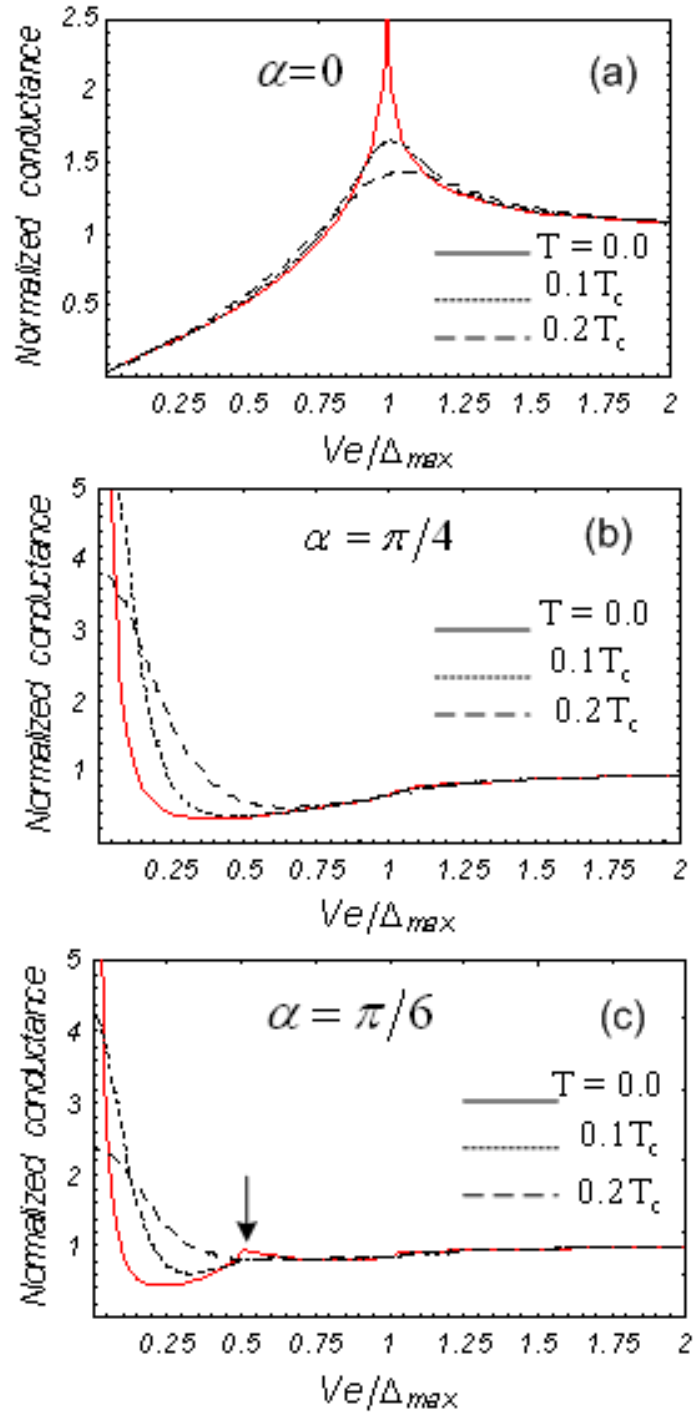
Figure 4.3: The plots of normalized conductance at different temperature $T = 0.0$, $0.1T_c$, $0.2T_c$, and with different angle $\alpha = 0$, $\pi/4$, $\pi/6$ for the high strength barrier Z=3.0.

Chapter V

Conclusion

In this thesis, the current and conductance spectra of normal metal-insulator-d-wave superconductor are calculated using the BTK formalism. In this approach, the dependence of the tunneling spectroscopy on the barrier strength, the interface orientation, and the temperature can be examined. In the high transmission limit, the conductance spectra indicate that the Andreev reflection dominates at small applied voltage. The normal reflection dominates in the low transmission limit.

The dependence of the tunneling conductance spectrum on the crystallographic orientation is found to be very useful in determining the magnitude of the energy gap in the momentum space. It is found that, in general, there are three distinctive features in the conductance spectra of d-wave superconductors. These features occur at maximum gap at zero voltage and at the voltage corresponding to the energy gap of the state with the momentum parallel to the interface normal of the junction. This features are very distinctive form those of the junction with low transparency at low temperatures. The existence of last feature implies the ability to use the NIS tunneling spectroscopy as a tool to determine the magnitude of the gap at different points on the Fermi surface.

All the features found at zero temperature tend to be broadened and smeared out at higher temperatures. The width of the zero-bias conductance peak is broadened when the temperature is increased, whereas the height of the peak is decreased.

In the future, it is interesting to explore how the increment in width and

decrease in height vary quantitatively with temperature. The effect of finite temperatures implies that to use the NIS tunneling spectroscopy as a tool to measure the magnitude of the gap at different points on the Fermi surface, one should make sure that the experiment should be done at lower temperatures than 10% of T_c.

References

References

Andreev, A. F. (1964). **Sov. Phys. JETP.** 19, 1228.

Bang, Y., and Choi. H-Y. (2000). Tunneling spectroscopy of the underdoped high-T_c superconductors. **Phys. Rev. B** 62, 11763.

Bardeen, J., Cooper, L. N., and Schriffer, J. R. (1957). **Phys. Rev.** 108, 1175.

Blonder, G. E., Tinkham, M., and Klapwijk, T. M. (1982). Transition from metallic to tunneling regimes in superconducting microconstrictions: Excess current, charge imbalance, and supercurrent conversion. **Phys. Rev. B** 25, 4515.

Demers, J., and Griffin, A. (1971). Tunnleing in the normal metal-insurator-superconductor geometry using the Bogoluibov equation of motion. **Phys. Rev. B** 4, 2202.

Gagnon, R., Pu, S., Ellman, B., and Taillefer, L. (1997). Anisotropy of Heat Conduction in $YBa_2Cu_3O_6$ **Phys. Rev. B** 63, 104510.

Giaever, I. (1960). Energy gap in superconductors measured by electron tunneling. **Phys. Rev. Lett.** 5, 147.

Giaever, I., and Megerle, K. (1961). Study of superconductor by electron tunneling. **Pys. Rev.** 122, 1101

Hu, C-R. (1994). Midgap surface states as a novel signature for $d_{x_a^2-x_b^2}$ -wave superconductivity. **Phys. Rev. Lett.** 72, 1526.

Kashiwaya, S., Tanaka, Y., Koyamagi, M., and Kajimura, K. (1996). Theory for tunneling spectroscopy of anisotropic superconductors. **Phys. Rev. B** 53, 2667.

McMillan, W. L., Rowell, J. M. (1969). **in superconductivity**, edited by R. D. Parks. (Marcel-Dekker, Newyork). Vol. 1, p. 561.

Pairor, P., and Walker, M. B. (2002). Tunneling conductance for d-wave superconductors: Dependence on crystallographic orientation and Fermi surface. **Phys. Rev. B** 65, 064507.

Parks, R. D. (1996). **Superconductivity**. (Vols. 1).

Raner, Ch., Revaz, B., Genoud, J. Y., Kadowaki, K., and Fischer, Ø. (1998). Pseudogap preccusor of the superconducting gap in uder and overdoped $Bi_2Sr_2CaCu_2O_{8+\delta}$. **Phys. Rev. Lett.** 80, 149.

Taillefer, L., Lussier, B., Gagnon, R., Behnia, K., and Aubin, H. v'e. (1997). Universal Heat Conduction in $YBa_2Cu_3O_{6.9}$ **Phys. Rev. Lett.** 79, p. 483-486.

Tanaka, Y., and Kashiwaya, S. (1994). Zero bias conductnce peak (ZBCP) is known to occur in junction. **Phys. Rev. Lett.** 72, 1526.

Tanaka, Y., and Kashiwaya, S. (1995). Theory of tunneling spectroscopy of d-wave superconductors. **Phys. Rev. Lett.** 74, 3451.

Tinkham, M. (1996). **Introduction to superconductivity**. (2nd ed.). McGraw-Hill, Inc.

Tsuei, C. C., and Kirtley, J. R. (1998). **Implications of pairing symmetry for hihg-temperature superconductivity in the cuprates**. Chinese Journal of Physics. 36, p.2-11.

Walker, M. B., and Lueettmer-Strathman. J. (1996). Josephson tunneling in high-T_c superconductor. **Phys. Rev. B** 54, 588.

Walker, M. B., and Pairor, P. (1999). Discrete-lattice model for surface bound state and tunneling in d-wave superconductor. **Phys. Rev. B** 59, 1421.

Wei, J. Y. T., Tsuei, C. C., Van Bentum, P. J. M., Xiong, Q., Chu, C. W., and Wu, M. K. (1998). Quasiparticle tunneling specrta of the high T_c mercury cuprates: Implications of the d-wave two-dimensional van Hove Scenario. **Phys. Rev. B** 57, 3650.

Wei, J. Y. T., Yeh, N-C., Garrigus., and Strasik. (1998). Directional tunneling and Andreev reflection on $YBa_2Cu_3O_{7-\delta}$ single cristals: Prenominance of the d-wave pairing symmetry verified with the generalized Blonder, Tinkham, and Klapwijk theory. **Phys. Rev. Lett**. 81, 2542.

Wolf, E. L. (1985). **Principles of Electron Tunneling Spectroscopy**. Oxford university Press, NewYork.

Wollman, D. A., Van Harlingen, D. J., Lee, W. C., Ginsberg, D. M., and Leggtt, A. J. (1993). Experimental determination of the superconducting pairing state in YBCO from the phase coherence of YBCO-Pb dc SQUIDs. **Phys. Rev. Lett.** 71, 2134.

Xu, J. H., Miller, J. H., and Ting, C. S. (1996). Conductance anomalies in a normal-metal-d wave superconductor junction. **Phys. Rev. B** 53, 3604.

Curriculum Vitae

NAME : Lemthong Lathdavong

SEX : Male

NATIONALITY : Laosian

PERSONAL : Married; Born in Vientiane Province, Lao P.D.R. Fluent in English, Thai, Lao.

EDUCATIONAL BACKGROUND :

- High School 1984, Vientiane Province of Lao P.D.R.

- B.Sc. 1988 (Mathematics-Physics), Pedagogy Institute of Lao P.D.R.

- Master's Degree 2002 (Physics), Institute of Science, Suranaree University of Technology, Thailand.

WORK EXPERIENCE :

- 1988-1995 Lecturer in physics at Department of Mathematics-Physics, Pedagogy Institute of Lao P.D.R.

- 1995-2000 Lecturer in Physics at School of Foundation Studies and Department of Physics Faculty of Science (National University of Laos).